Angle Resolved Scattering Combined with Optical Profilometry as Tools in Thin Films and Surface Survey

K. Marszałek[a], N. Wolska[b,c] and J. Jaglarz[b,*]

[a]AGH University of Science and Technology, al. A. Mickiewicza 30, 30-059 Krakow, Poland

[b]Institute of Physics, Cracow University of Technology, Podchorążych 1, 30-084 Kraków, Poland

[c]Elkom Trade S.A., Targowa 21, 27-400 Ostrowiec Świętokrzyski, Poland

The work presents an application of two scanning optical techniques, i.e. optical profilometry and angle resolved scattering method. The first method measures the light reflected from a film during scan of the surface, while the second method measures light intensity as a function of the scattering angle. The angle resolved scattering and optical profilometry measurements, being complementary to the atomic force microscopy, give information about surface topography. Scattered radiation measured by angle resolved scattering and optical profilometry is a function of height and slope of microfacets. The analysis of images allows to determine the most important statistic surface parameters, like roughness, height distribution and autocorrelation length, in large wavelength range by the determination of power spectral density function. The fast Fourier transform of angle resolved scattering and optical profilometry images permits to determine the distribution of surface features in the inverse space, such as periodicity and anisotropy. In this paper the results obtained for porous SiO_2, SiO_2–TiO_2 blends, TiN and polymer thin films have been presented. The paper demonstrates the usefulness of the angle resolved scattering and optical profilometry for the surface and volume thin film inspection.

1. Introduction

Light scattering from optical thin films and devices has increasingly become an important factor in applications requiring high precision control. Also, light scattering losses have crucial impact on the performance quality of optical thin films [1, 2] and devices [3, 4]. The study of light scattering from optical thin films can provide useful information on thin film morphology. If layers are thin and flat the basic parameters describing studied films (i.e. thickness and refractive index) may be determined from the analysis of reflection spectra. Optical methods use for this purpose the specular part of radiation from the sample. In particular, the spectroscopic ellipsometry is accurate technique for determination of thickness and refractive index of thin films [5, 6]. The basic ellipsometric equation utilizes the Fresnel formulae to determine optical and geometrical parameters of thin layers.

However, in many real films except coherent specular scattering, the non-directional incoherent scattering may occur. There are two types of non-specular light scattering in optical thin films. The first one is the surface scattering, which results from irregularities appearing on the film–substrate and film–air interface [7]. The second one originates from scattering occurring in the volume of films [8]. Light scattering in bulk of optical thin films results from scattering centers with refractive index different than the film [9]. If the variations in layer surfaces and in the bulk are mild, then they can be characterized by weak single scatter events, as in the case of smooth surface topography, where the scattering is caused by particles embedded in the bulk of a film. Then, one can consider the total diffuse reflection as the sum of surface I_s and volume scattering I_v, namely $I_{tot} = I_v + I_s$. Thus, diffuse films, from an optical point of view, show the same behavior as layers with rough boundaries.

The work presents an employment of two scanning optical techniques i.e. optical profilometry (OP) and ARS (angular resolved scattering) techniques. The first method measures the light reflected from a film during scan of the surface, while the second method measures light intensity as a function of the scattering angle. Arbitrarily, one may separate ARS technique into bidirectional reflection distribution function ($BRDF$) method [7] used for film topography measurements and small angle light scattering ($SALS$) applied in bulk scattering investigation [9].

The only difference between $BRDF$ and $SALS$ method is the range of incidence and scattered angles θ_i and θ_s respectively. In $BRDF$ the angle θ_i is usually fixed at larger than 45° values and angles θ_s are altered in wide range angles higher than 45°. In SALS type of measurements incident angle θ_i is close to zero and scattered angle is usually lower than 15°.

Measurements of optical reflectance by means of the classical reflectometry inform us about optical properties on a large area, i.e. of the order of 0.1 to 2 cm^2. Results obtained on a much less scale will be similar if coatings and surfaces are homogeneous over the investigated area and inside the layers. For inhomogeneous surfaces, when topographic or material non-uniformities appear, the results differ from tens μm to several mm, the measurements taken from the integrating sphere and

---

*corresponding author; e-mail: pujaglar@cyfronet.pl

standard reflectometry give rather an average reflectance over a larger scale of the reflected samples.

The scattered radiation measured by OP is a function of height of irregularities and slope of microfacets, but the sensitivity of this method results mainly from detection of the slope change [10]. The presence of long lateral irregularities is often caused by manual or mechanical treatments and may have a periodical nature. The short spatial waves result rather from the random process of the surface formation and their contribution to the total profile is easy to determine from atomic force microscopy (AFM) technique.

Optical profilometry measures specularly reflected light from the sample "in point". The resolution of OP depends on beam diameter which changes from 1 μm to 1 mm. In this work we present the results of profilometric studies. The long spatial wavelength irregularities detected in OP investigations may substantially contribute to the total roughness. The ARS and OP measurements complete the topography description in long spatial wavelengths.

Two main theories were developed to analyze light scattering in optical thin films: the scalar [11] and the vector theory [12].

Scalar light scattering theory based on the Kirchhoff–Beckman approximation provides the total integrated scattering (TIS) formula. TIS is defined as the ratio of diffuse to specular intensity of scattered radiation. TIS describes the relationship of surface roughness and light scattering [13]. The well known TIS formula can be expressed in the first approximation as

$$TIS = \exp\left[-\left(4\pi\sigma\right)/\lambda\right)^2\right], \tag{1}$$

where σ is the rms surface roughness and λ is the wavelength of light illuminating the sample. The validity of the above relation is fulfilled for $\sigma \ll \lambda$. The simple way to determine TIS parameter is to use the integrating sphere [14].

Vector scattering theory is based on the first-order perturbation model and valid for small roughness (rms) σ. In contrast to scalar approaches, it includes the polarization properties of both scattered and incident light. Vector theory in the Rayleigh–Rice [15] and the Rayleigh–Debye approximation [16] can be applied for surface and bulk of light scattering phenomena occurring in thin films.

In surface vector theory some function describing surface in topographical terms must be defined.

Real surfaces most often are described by statistical function, namely power spectral density (PSD) function. PSD expresses the roughness power per unit spatial frequency over the sampling length [7].

The PSD is presented as a function of spatial frequency f:

$$f = \frac{\sin(\theta_s) - \sin(\theta_i)}{\lambda}, \tag{2}$$

where angles θ_i and θ_s are incident and scattering angle, respectively.

PSD function is commonly evaluated by processing mechanical profilometer and/or AFM images [1]. If the values of PSD are known, one can determine the statistical parameters, such as the root-mean square (rms) roughness σ, slopes and the autocorrelation length by using the so-called ABC model which describes PSD in a simple analytical form [7, 14]:

$$PSD(f) = A[1 + (Bf)^2]^{-C/2}, \tag{3}$$

where A, B and C are model parameters related to basic quantities characterizing a surface, i.e. A is a PSD value for low frequency, $B/2\pi$ is the correlation length and C determines the type of power law in high spatial frequency. The C parameter qualifies type of random distribution of irregularities. For the special case $C = 2$ or $C = 4$, the distribution of $PSD(f)$ is Lorentzian or Gaussian, respectively. The ABC model is applicable to single surface or interface. The function describing surface topography in spatial wavelengths is autocovariance function [1].

In order to determine the PSD function $BRDF$ method has been used [17]. $BRDF$ method measures the differential power of scattered beam dP per solid angle of receiver aperture dΩ in the θ_s direction and per incident power P_i coming from the θ_i direction. The angles used in $BRDF$ have been shown in Fig. 1.
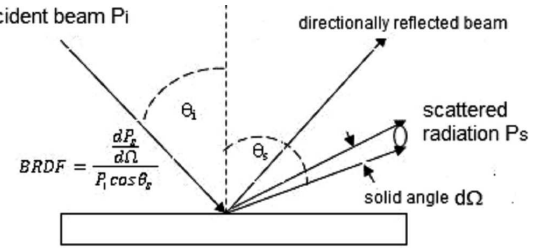

Fig. 1. The angles defined in $BRDF$ technique.

Practically, dP/dΩ is equal to the measured scatter power P_s per acceptance angle Ω of a detector, namely

$$BRDF = \frac{\mathrm{d}P/\mathrm{d}\Omega}{P_i \cos\theta_s} = \frac{P_S}{P_i \Omega \cos\theta_S}\left[sr^{-1}\right]. \tag{4}$$

If the surface under consideration is relatively flat, one can use the Rayleigh–Rice vector perturbation theory yielding a simple dependence between the scattered radiation expressed by $BRDF$ and PSD functions [1, 7]:

$$BRDF = \frac{16\pi^2}{\lambda^2}\cos\theta_i\cos\theta_s Q PSD(f), \tag{5}$$

where Q is a factor depending on polarization state of the light source and optical constants, and λ is the light wavelength. This relationship allows one to extract the topographic structure of a single surface from either $BRDF$- or PSD studies, since both functions are proportional to each other. Equation (5) is the basic in determination of surface parameters from angular scattering measurements and may be applied to relatively smooth surfaces for all kinds of films, including strongly absorbing ones (e.g. metallic films).

However, if a thin film is deposited on a rough surface, the *BRDF* depends on the profiles of upper and bottom interfaces. Then, even for a slightly absorbing or transparent thin film, the *BRDF–PSD* relationship is much more complicated, in particular, when a partial correlation between interfaces occurs. For completely correlated the top and bottom film surfaces the factor Q is optical functions of film/air- and film/substrate interfaces which represents reflection from a film.

Volume scattering is a part of elastic scattering caused by the film bulk. It is assumed that there is no energy loss accompanying the scattering and that the scattering bulk is spherically symmetric. The scattering light in a bulk is described by formula [19]:

$$I_s = a^3 B / (1 + k^2 a^2 s^2)^2, \qquad (6)$$

where s and k are the scattering and wave vector, respectively: $s = 2\sin(\theta/2)$, $k = 2\pi/\lambda$.

The parameter B is the scattering factor, and a is correlation length describing the distance between refractive index fluctuation caused by the scattering centers. The contribution of volume scattering to the total diffuse reflectance is larger for small angles of scattering. This is significant mainly in translucent materials with a small extinction coefficient.

Surfaces and layers can be described in different ranges of space wavelengths (or frequencies). Spatial short waves cause scattering into high angles, while long ones scatter into low angles, close to the specular beam. Thus scattering is bandwidth-limited and only scattering caused by a certain range of surface roughness frequencies can be detected by an instrument.

The attenuation of light described by the loss function is defined as the inverse distance, when the intensity of specular light decreases e-fold due to scattering by particles and the absorption process. Then the total loss coefficient is equal to $s_t = a + s_v$, where a is the absorption and s_v is the volume scattering coefficient.

2. Experimental setups

For quantitative and qualitative thin film inspection the novel nonstandard setups have been applied. They comprise several original solutions useful in a wide range of films with different optical constants, thicknesses and roughness.

BRDF measurements have been performed with an automatic home-made scatterometer setup. It consists of a 635 nm laser diode as a light source with the beam diameter of 2 mm mounted on a goniometric table with resolution of 0.01 deg. The light scattered at the sample surface is measured with a Si photodiode detector. The rotations are obtained by a computer controlled step motors. For a fixed angle of incidence, the intensity scattered in the plane of incidence have been measured by varying the detector orientation. All measurements have been carried out with the *s*-polarized incident beam. In any case, the sample surface size has been much larger than the beam diameter [20]. Moreover, the minimal illuminated area (4 mm²) has been large enough for statistical

description of the surface. The scheme of *BRDF* setup is shown in Fig. 2.
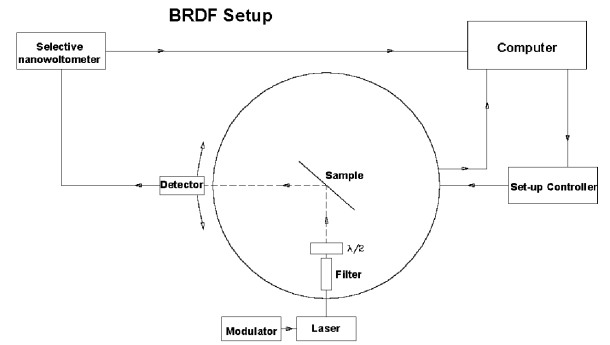

Fig. 2. Scheme of *BRDF* setup.

SALS measurements were carried out with an automatic scatterometer. It consisted of the 635 nm laser diode as the light source. The CCD ruler with 512 diode elements was applied for scattered light detection. The resolution angle per pixel was equal to 0.06 which was suitable value for that type of measurements. The scattering angles θ_s ranged from 1° to 13°. The measurements were done in the plane of light incidence with the *s*-polarized incident beam.
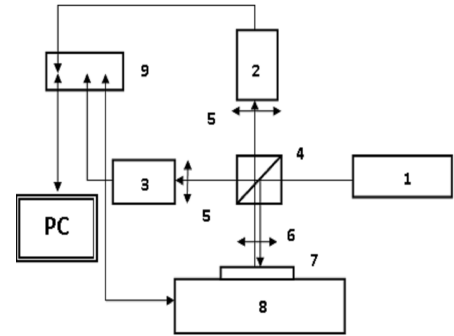

Fig. 3. Scheme and picture of optical profilometer: 1 — laser diode ($\lambda = 635$ nm), 2,3 — detectors, 4 — beam splitter, 5 — collecting lens, 6 — objective, 7 — sample, 8 — XY stage, 9 — controlling/collecting unit.

The scheme of OP has been shown in Fig. 3 [10]. OP is a multifunctional experimental setup for surface topography investigations. It works in two modes. The first — specular mode, employs the laser diode with wavelength $\lambda = 635$ nm as a light source with the collimating system allowing to achieve a 12 μm diameter light beam. It allows to obtain the optical map of surface with a 12 μm lateral resolution. In the second mode the reflection probe R200-7 mode is utilized. The XY positioning stage is actuated by lead screw step motor. It allows to scan 20 mm × 20 mm surface area with step of 20 μm.

3. Result and discussion

The optical scanning method could be applied in thin slightly rough films which additionally exhibit optical dif-

fusion in the bulk. The *BRDF* study performed at zero angle of incidence allows us to separate optical losses caused by volume or surface scattering from total light scatter. Such diffusive behavior can be observed in polymer layers applied in optoelectronic devices.
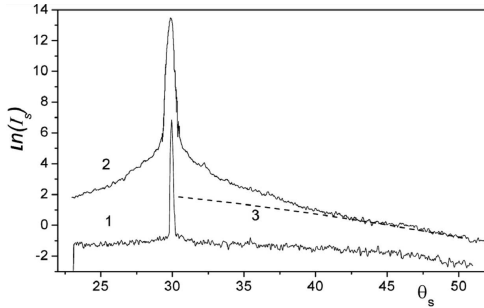

Fig. 4. log (ARS) for the BK-7 glass with the surface roughness $\sigma = 3$ nm (curve 1) and a relatively thick PPI film (curve 2).

Figure 4 shows the log(ARS) results performed for BK-7 glass with the surface roughness $\sigma = 2.9$ nm (curve 1) and a relatively thick polymer film (curve 2). The difference of shapes of the presented curves indicates that below angles smaller than the Brewster angle θ_B, scattered light comes from the volume as well as from the surface of the film. This difference is easy to explain, namely: if the bottom surface is flat (as for glass or polished Si substrate), the radiation, coming from refractive index fluctuations or from scattering centers, is scattered into an angle θ_s which may be larger than θ_B. In this case, all radiation, scattered at angles $\theta_\sigma > \theta_B$, is internally reflected. Thus for these angles, the light scattering coming from the upper surface of films is only produced by film irregularities.

That allows to extrapolate for larger scattering angles the light scattered by the surface from total scattering signal. That is demonstrated by curve 3 in Fig. 4. The volume scattering is a result of subtraction of the surface scattering from the total scattering.
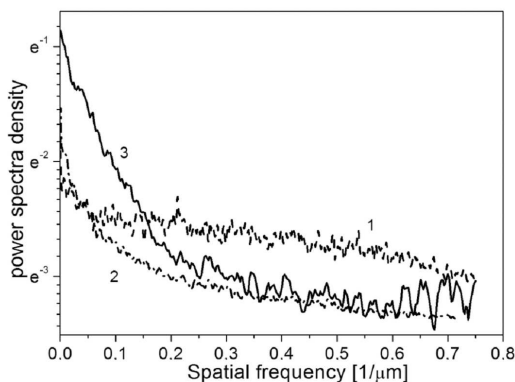

Fig. 5. log–log *PSD* versus spatial frequency f of irregularities for sample from Table.

If bulk scattering does not occur the optical losses originate from surface and interface only. In that case it is allowed to determine the roughness σ, autocorrelation length T and power coefficient C of high distribution law from *BRDF* measurements using formula (3). Figure 5 shows determined *PSD* function for polished silicon (curve 1), thermally obtained SiO_2 on the same Si substrate (curve 2), porous silica films obtained by sol–gel technique [21] (curve 2), respectively. The values of σ, T and C calculated from (6) for Si and SiO_2 have been presented in Table. Also in Table the roughness values obtained from AFM study have been placed.

TABLE
Topographic parameters calculated from *PSD* function for samples described in text.

Sample	d [nm]	Roughness AFM σ [nm]	Roughness $BRDF$ σ [nm]	A_{corr} [nm]	C
polished Si	–	0.7	1.3	273	3.6
SiO_2 on Si	12	0.5	0.9	289	3.9
porous silica on Si	625	0.2	7.7	192	2.0

As one may notice in Table irregularities of films with porous SiO_2 have smaller autocorrelation length. Therefore shorter spatial wavelengths contribute with larger fraction to total roughness than in cases of Si and thermal SiO_2. Therefore autocorrelation lengths T for layers 1 and 2 are bigger than for thermally obtained silica. *PSD*s obtained for silicon before and SiO_2 on Si after annealing are very similar. It results from the identity of upper and lower interfaces of SiO_2 film. Values of σ determined from AFM and *BRDF* measurements are similar, however, roughness calculated from *BRDF* study is larger. As a matter of fact in *BRDF* we measure scattered radiation from a much bigger surface area than in AFM. Abnormal light scattering from short space wavelengths shows that beside scattering due to surface irregularities there is other different mechanism of light scattering. It is due to the presence of pores in the film bulk. Significant differences between the roughness determined by the AFM and BRDF (Table) can be explained by the presence of light scattering at times.

Additionally, the OP measurements for absorbing and transparent thin films have been performed. It allows to determine thickness variation upon the plane position of measured point for some samples. Thickness variation measured by OP is shown in Fig. 6. The DLC layer was obtained by the use of ion beam assisted deposition (IBAD) method [22]. In Fig. 6 one may observe the radial decrease of film thickness from ion central bombarding axis position of sample to external areas of sample.

In some processes the thickness of film may be irregularly distributed. We present as an example of such effect the TiO_2 layer created on TiN substrate during thermal annealing in temperature 1200–1400 K. The OP profile of TiN surface subjected thermal oxidation is shown in Fig. 7.
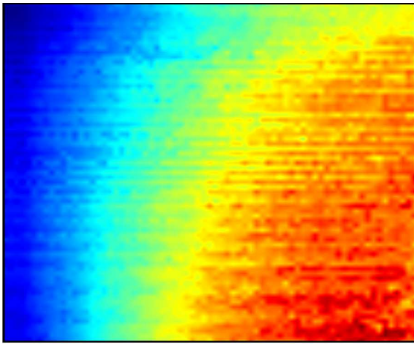
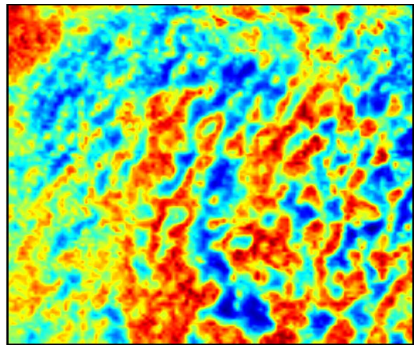Fig. 6. OP profile of DLC film on Si produced by the use IBAD technique.

Fig. 7. OP profile of TiO$_2$ film created during the TiN annealing.
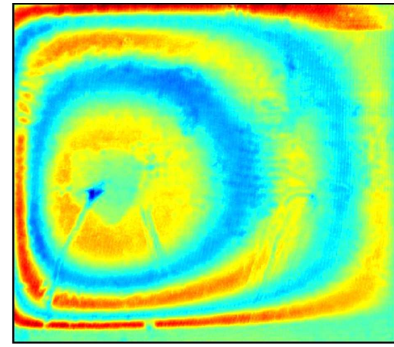

Fig. 8. OP profile of a PPI on the glass substrate film created in CVD process.
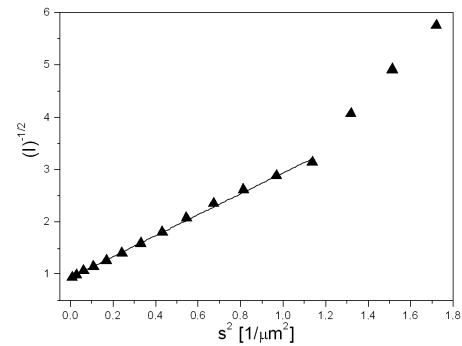
Fig. 9. SALS normalized intensity vs. scattering vector for PPI layer.

The red areas in Fig. 7 correspond to thicker TiO$_2$ layer, while blue ones are spots with lower thickness of oxide films. The thickness variation shows rather statistical distribution over the sample area. Also, for polymer films optical profilometry proved many advantages. They show an even larger variety of surface and volume phenomena than non-organic layers. As an example the optical profile of polyazomethine (PPI) thin film obtained in CVD technology [23] has been shown in Fig. 8. The light entering to PPI film was scattered by refractive index fluctuations and coming back through PPI layer–air interface under solid angle less than 2π. The film thickness (the thicker the film, the larger the number of scattering centers and the greater intensity of backscattered light). The circular lines of reflection maxima originate from surface points of largest thicknesses of PPI film. As one may notice, the shape of maxima reflection envelopes is changing from circular in centre of the sample to rectangular for points adjacent to sample confines.

Because the PPI film exhibited volume scattering also the SALS investigation was performed. For small values of s, the formula (6) may be transposed to a linear dependence of the inverse square root of the normalized intensity vs. the square of the scattering vector s. Figure 9 shows the experimental SALS data transformed according to the above description.

Using a linear fit to the transposed SALS data for small values of the scattering vector, the autocorrelation length $a = 7.5$ μm and the scattering factor $B = 5.43 \times 10^{-2}$ μm^{-3} have been estimated.

Optical profilometry could be applied to waviness detection occurring on sample surface. As an example, on Fig. 10a the OP profile of crystalline silicon subjected to etching during the time 40 min in 25% solution of KOH have been shown.
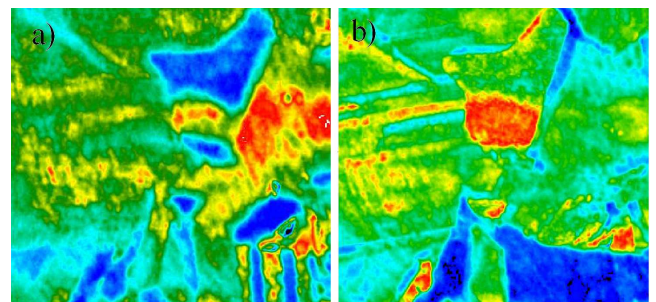

Fig. 10. The OP profile of etching silicon surface: a) left — the profile obtained for normal incident, b) — axis of the light is inclined at the angle of 15° to normal.

The profile was obtained for normal incident beam. In this case, the probe measure directionally reflected and diffusive scattered light. If the axis of the light is inclined
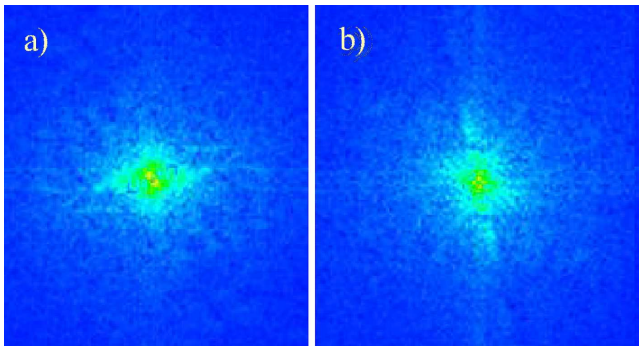
Fig. 11.   FFT profiles of images presenteds in Fig. 10a and b.

at the angle of 15° to the sample axis, the probe records only nonspecularly scattered light. The measured profile at angle of 15° for the same sample of etched silicon is shown in Fig. 10b.

In this case, the diffusely reflected light is measured, so recorded profile shows the image of the scattered light coming mainly from the the the sample microroughnes.

In Fig. 11a and b the Fourier transform profiles from Fig. 10a and b have been shown respectively. The transforms of optical profile image allows in easy way to determine the periodicity and anisotropy of the studied surfaces

4. Conclusion

The work presents an employment of two scanning optical techniques i.e. OP and ARS method in thin film investigations. The first method measures the light reflected from a film during scan of the surface, while the second method measures light intensity as a function of the scattering angle. The ARS and OP studies allow to get information about surface topography in short spatial frequencies. The scattered radiation measured in OP is a function of height and slope of irregularities, but sensitivity of OP studies results mainly from the detection of the slope change. The presence of long lateral irregularities is often met in polymer technology and it can have a periodical nature. Short spatial waves result rather from a random process of the surface formation and their contribution to the total profile is easier to be determined by AFM.

ARS and OP investigations enable one to find many interesting features concerning surfaces in a much larger area than AFM technique. From ARS study one is allowed to find most important statistical parameters characterizing single surface or film-substrate interface as roughness σ correlation length L and high distribution function. In OP study the image analysis performed by the use of fast Fourier transform (FFT) allows one to find distribution of features in the inverse space, like periodicity and anisotropy.

References

[1] J.M. Elson, J.M. Bennett, *Introduction to Surface Roughness and Scattering*, 2nd ed., OSA, Washington 1999.

[2] P. Winkowski, K. W. Marszalek, *SPIE Proc.* **8902**, 890228 (2013).

[3] R.H. Dennard, Jin Cai, A. Kumar, in: *Handbook of Thin-Film Deposition Processes and Techniques*, Ed. K. Seshan, 2nd ed., William Andrew Publ., Norwich 2002, p. 3.

[4] K. Marszalek, P. Winkowski, J. Jaglarz, *Mater. Sci. Poland* **32**, 80 (2014).

[5] R.M.A. Azzam, N.M. Bashara, *Ellipsometry and Polarized Light*, North-Holland, Amsterdam 1987.

[6] J. Jaglarz, T. Wagner, J. Cisowski, J. Sanetra, *Opt. Mater.* **29**, 908 (2007).

[7] J.C. Stover, *Optical Scattering: Measurement and Analysis*, 2nd ed., SPIE Press, Bellingham 1995.

[8] H.C. van de Hulst, *Light Scattering by Small Particles*, Dover, New York 1981.

[9] F. Scheffold, R. Cerbino, *Coll. Interface Sci.* **12**, 50 (2007).

[10] J. Jaglarz, *Topography Description of Surfaces and Thin Films by Fourier Transform, Obtained from Non-Standard Optical Measurements in Fourier Transforms Theory and Applications*, Intech Open Access Publisher, Rijeka 2011.

[11] P. Beckmann, B. Spizinochino, *The Scatering of Electromagnetics Waves from Rough Surfaces*, Pergamon Press, Oxford 1963.

[12] S.O. Rice, *Pure Appl. Math.* **4**, 351 (1951).

[13] A. Arecchi, K.A Carr, *Guide to Integrating Sphere Theory and Application*, Labsphere Technical Guide, 1997.

[14] J.A. Ogilvy, *Theory of Wave Scattering from Random Rough Surfaces*, Hilger/IOP, 1991.

[15] J.M. Elson, J.M. Bennet, *Opt. Eng.* **18**, 116 (1979).

[16] P. Debye, *J. Appl. Phys.* **15**, 388 (1944).

[17] J. Jaglarz, *Thin Solid Films* **516**, 8077 (2008).

[18] D. Ronnow, T. Eisenhammer, T. Roos, *Solar En. Mater. Solar Cells* **52**, 37 (1998).

[19] J. Zhou, J. Sheng, *Polymer* **38**, 3727 (1997).

[20] Ł. Zięba, J. Jaglarz, M. Dąbrowski, R. Duraj, J. Cisowski, J. Jurusik, *Rev. Adv. Mater. Sci.* **15**, 63 (2007).

[21] P. Karasiński, C. Tyszkiewicz, R. Rogoziński, J. Jaglarz, J. Mazur, *Thin Solid Films* **519**, 5544 (2011).

[22] J. Esteve, M.C. Polo, G. Sanchez, *Vacuum* **52**, 133 (1999).

[23] J. Jaglarz, J. Cisowski, H. Czternastek, J. Jurusik, M. Domański, *Polimery* **1**, 54 (2009), (in Polish).